

Global versus local adaptation in fly motion-sensitive neurons

Peter Neri* and Simon B. Laughlin

Department of Zoology, University of Cambridge, Downing Site, Cambridge CB2 3EJ, England

Flies, like humans, experience a well-known consequence of adaptation to visual motion, the waterfall illusion. Direction-selective neurons in the fly lobula plate permit a detailed analysis of the mechanisms responsible for motion adaptation and their function. Most of these neurons are spatially non-opponent, they sum responses to motion in the preferred direction across their entire receptive field, and adaptation depresses responses by subtraction and by reducing contrast gain. When we adapted a small area of the receptive field to motion in its anti-preferred direction, we discovered that directional gain at unadapted regions was enhanced. This novel phenomenon shows that neuronal responses to the direction of stimulation in one area of the receptive field are dynamically adjusted to the history of stimulation both within and outside that area.

Keywords: vision; insect; neural coding; directional gain

1. INTRODUCTION

The effect of motion adaptation on perception is easily demonstrated by viewing a pattern moving in one direction for 40–60 s, followed by a physically static one: the latter appears to move in a direction opposite to the former (Addams 1834; Mather *et al.* 1998). This after-effect, the waterfall illusion, is not unique to humans: elegant behavioural work has shown that it is also experienced by flies (Götz & Wenking 1973; Srinivasan & Dvorak 1979), indicating that motion adaptation is also relevant to these animals (Clifford & Langley 1996). In flies, the physiological counterpart of this phenomenon can be found in motion-sensitive neurons in the third visual neuropile (lobula plate), most of which sum motion signals across large areas of visual space (Hausen 1984; Krapp & Hengstenberg 1996; Egelhaaf *et al.* 2002). Similarly to macaque MT neurons (Kohn & Movshon 2003, 2004), these cells adapt their response characteristics to prolonged stimulation (Srinivasan & Dvorak 1979; Maddess & Laughlin 1985; de Ruyter van Steveninck *et al.* 1986; Fairhall *et al.* 2001).

In mammalian (Movshon & Lennie 1979; Carandini & Ferster 1997) and fly (Harris *et al.* 2000) motion-sensitive neurons, adaptation has two main effects on contrast response curves: (1) a change in mean firing rate shifts the entire curve up or down; and (2) a change in gain. Because the shift is a subtractive process that opposes recent activity in the cell, it is directional and can explain the waterfall illusion (Barlow & Hill 1963; Maffei *et al.* 1973; Srinivasan & Dvorak 1979). The change in contrast gain is a multiplicative process that is non-directional because it is driven by motion in any direction (Harris *et al.* 2000). A major component of adaptation is local (Maddess & Laughlin 1985), for its effects are confined to the adapted region, and a similar result has recently been reported for MT neurons (Kohn & Movshon 2004).

Our experiments explored the spatial and directional dependency of adaptation more extensively, by measuring directional gain rather than contrast gain. Similarly to contrast gain (Harris *et al.* 2000), directional gain was equally reduced by motion adaptation in both preferred and anti-preferred directions when tested at the adapted location. When the test location was outside the adapted region, directional gain was reduced by motion adaptation in the preferred direction, but enhanced by motion adaptation in the anti-preferred direction. These new results show that each region of the receptive field is independently recalibrated by taking into account both local (within the region) and global (outside the region) features of previous stimulation.

2. MATERIAL AND METHODS

(a) *Electrophysiological recordings*

We recorded extracellularly from 10 V1 neurons and 20 H1 neurons (two tested subregions per neuron on average) in 29 blow flies (*Calliphora vicina*). There is one V1 and one H1 neuron in the hemisphere of each animal, and they are easily identified by their firing patterns and directional preference (Hausen 1984). The fly was immobilized with wax and positioned so that the monitor (ViewSonic PT795), driven by a VSG graphics card (Cambridge Research Systems) at 180 Hz, would cover roughly 78°×74° (width×height) of visual angle to the left eye (monitor was typically centred at an azimuth/elevation of roughly 40°/5°), and recordings were made in the contralateral (right) lobula plate.

(b) *Preliminary mapping of receptive field*

We used a vector white noise reverse correlation technique (Srinivasan *et al.* 1993), in which a large portion of the neuron's receptive field is stimulated with a lattice of Gabor patches locally moving in random directions at a constant speed of 23° s⁻¹. Each patch subtended roughly 19°×18° (100% contrast on a 38 Cd m⁻² mean luminance background, carrier spatial frequency 0.1 cycles deg⁻¹, standard deviation of Gaussian envelope 4°), and moved for 220 ms in

* Author for correspondence (pn@white.stanford.edu).

one of eight possible directions at cardinal and diagonal axes. Each presentation lasted for 6.6 s (30 different lattice samples). We used around 200 presentations per neuron. By correlating the random motion sequence with the firing pattern (Srinivasan *et al.* 1993) we derived vector maps (e.g. figure 1*a*).

(c) Adaptation protocols

For the experiments in figures 1 and 2, we selected a highly responsive subregion within the map for pre-testing, adapting and post-testing. During the pre-test, we presented a sequence of eight oval gratings (each grating subtending $16.5^\circ \times 15.5^\circ$, 30% contrast on a 52 Cd m^{-2} mean luminance background, carrier frequency $0.1 \text{ cycles deg}^{-1}$, speed 23° s^{-1} , duration 220 ms) within the test region, taking all eight possible directions in random permutation (overall duration of pre-test $8 \times 220 \text{ ms}$). Starting half a second after pre-test, we adapted for 4–6 s with a 100% contrast grating (with the same characteristics as the test), applied in one of the four possible configurations described in the main text (see figure 2*b–e*), and moving in either the neuron's preferred or anti-preferred direction (4×2 different conditions). The surround covered the entire monitor, except for an oval region of $19^\circ \times 18^\circ$ centred at the test region (this cut-out was slightly larger than the test). We also had a control condition during which nothing was presented during the adapting phase. We repeatedly presented these nine different conditions in fully randomized order, with a recovery interval of 12–20 s between them. For the experiment in figure 3, we selected two subregions within the map, and used only oval gratings with the same characteristics as those just described.

(d) Directional gain change

Contraction/expansion (along the response axis) of directional tuning curves is captured by Δgain (reported in figure 2*k–t*), defined as $g-1$, where g is the slope of the regression line that fits $f_{\text{post}} = \text{slope} \times f_{\text{pre}} + \text{intercept}$, with f_{pre} and f_{post} being the directional tuning curves measured before and after adaptation. This measure is similar to that used by Treue & Martínez-Trujillo (1999), except that they used fitted data for f rather than raw data. Our analysis avoids assumptions about the shape of the fitting curve, and more closely preserves the structure of the actual experimental data. The average correlation coefficient for the regression just described is 0.85 in both our V1 and H1 datasets. The Δgain metric is independent of shifts: whichever model is chosen for shifts, the results reported in figure 2 for Δgain do not change.

3. RESULTS

(a) Main effect

Our experimental design and main results are summarized in figure 1. Immediately after isolating a motion-sensitive neuron, we mapped its vector response field (Srinivasan *et al.* 1993; see §2). For example (figure 1*a*), the neuron H1 is preferentially responsive to rightward (back-to-front) motion, and sums inputs throughout its entire receptive field with no sign of spatial opponency or figure-ground structure (Hausen 1984; Krapp & Hengstenberg 1997). We selected a small area of high sensitivity within the map (circled in *a*) and, by pre-testing it with a rapid sequence of eight patches moving in different directions (similar to the circular grating in *b*, but of lower contrast), obtained

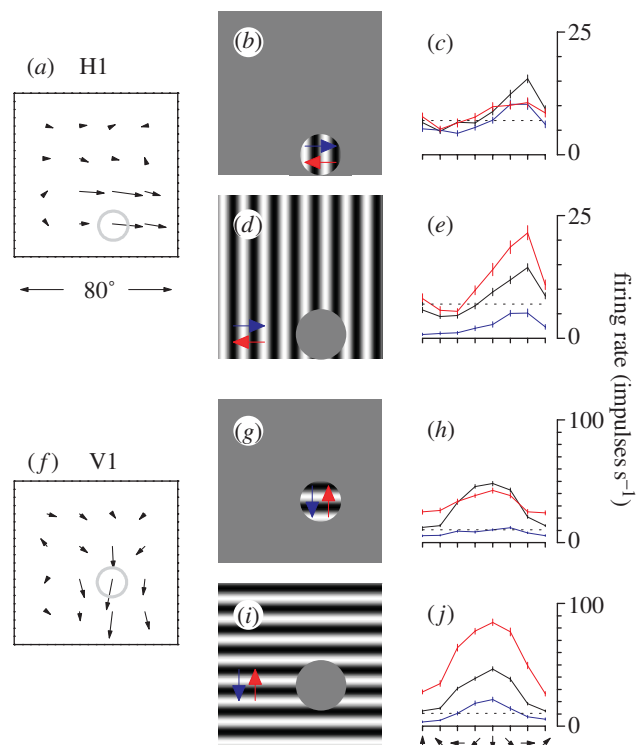


Figure 1. Directional gain enhancement effect. The vector response field of each neuron ((*a*) for an H1 neuron, (*f*) for V1) was mapped individually using a vector white noise technique (Srinivasan *et al.* 1993). A subregion within the map (circled) was selected as test region, and pre-tested with a 30% contrast circular grating (similar to the one in *b*), but of lower contrast) moving in eight different directions. This procedure yielded a directional tuning curve for the test region (black curve in *c*). Half a second after pre-test, a high-contrast adaptor was presented for 4–6 s. The adaptor could be restricted to the test subregion (*b*), or to the complementary region (*d*), and could move in either the preferred (blue) or anti-preferred (red) direction for the neuron. After the adapting phase, the selected subregion was post-tested using the same procedure used in the pre-test. Adaptation inside the test region reduces directional gain (vertical compression of the curve; Treue & Martínez-Trujillo 1999) for both directions (*c*). Adaptation outside the test in the anti-preferred direction leads to directional gain enhancement (expansion of the curve, *e*). (*a*)–(*e*) show results for a neuron (H1) preferring rightward (back-to-front) motion, (*f*)–(*j*) for one (V1) preferring downward motion. Error bars show ± 1 s.e.m. Dotted lines are baseline firing rates (in the absence of visual stimulation).

the directional tuning curve for that small area (black curve in *c*). We then stimulated the area with a high-contrast patch continuously moving for 4–6 s in either the preferred (blue) or anti-preferred (red) direction for the neuron (*b*). Immediately after the cessation of this adapting stimulus, we re-tested directional tuning using the stimuli and procedure of the pre-test. As shown by the coloured traces in *c*, prolonged stimulation with a high-contrast patch in either direction compresses the directional tuning curve along the response (y) axis (by 39% for the preferred, and 54% for the anti-preferred direction in the example shown). This compression is adaptation which, as described in H1 (Maddess & Laughlin 1985; de Ruyter van Steveninck *et al.* 1986), makes a significant contribution to efforts to understand short-term memory and coding efficiency in neural systems (Fairhall *et al.* 2001).

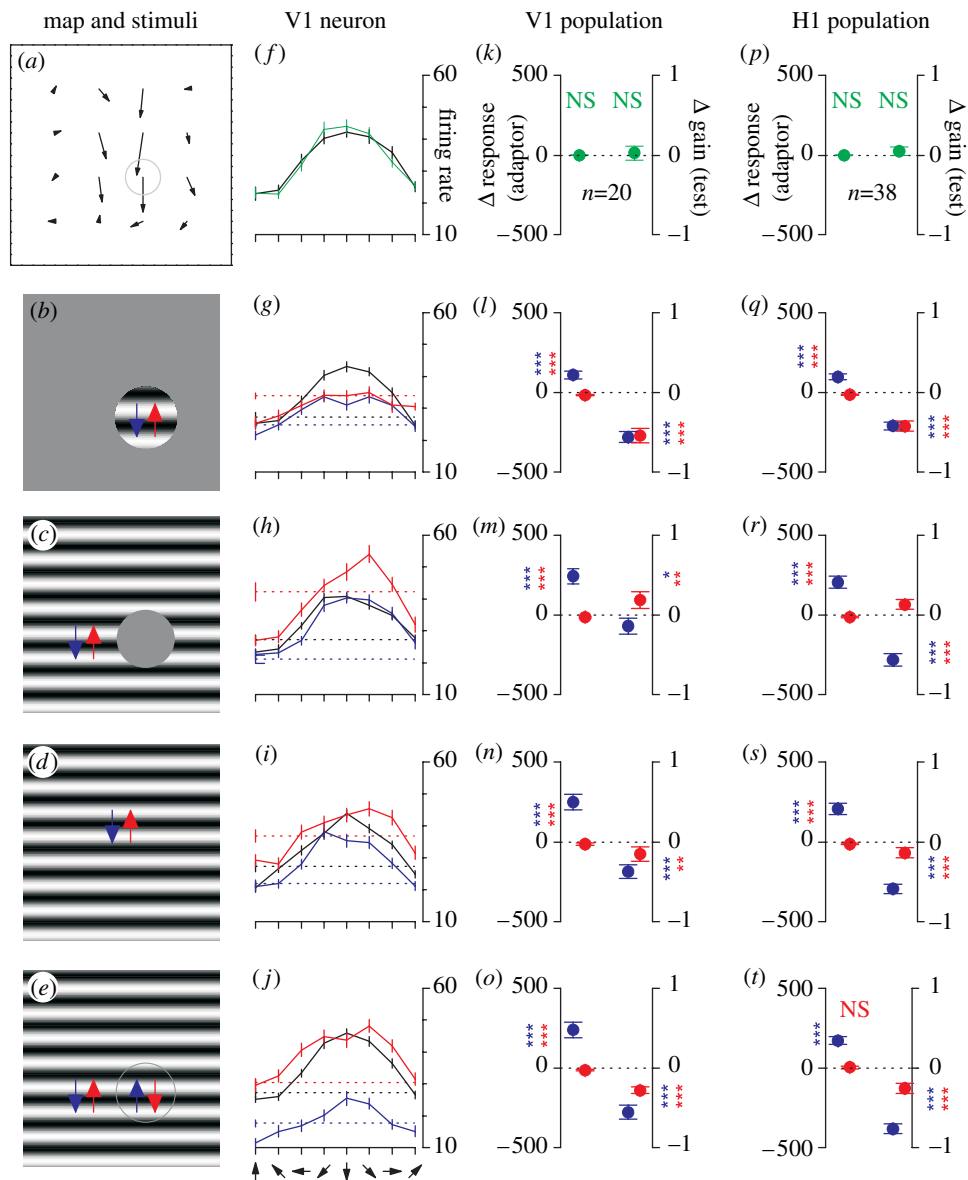


Figure 2. Full-field adaptors and population data; (a)–(j) show results for one V1 neuron. (a) The vector response field; (b)–(e) the four different adaptors used to stimulate it. (f) Directional tuning curves for pre-test (black) and post-test (green) at the location circled in (a), for a control condition in which no stimulus was presented during the adapting phase. Panels (g)–(j) show pre- and post-tests for the adaptors in (b)–(e) (same conventions as figure 1). Adaptors in (b) and (c) correspond to figure 1*g,i*. In (d)–(e), adaptors covered the whole monitor, with the circular region at test location moving in either the same (d) or opposite direction (e) with respect to the outside. Dotted lines in panels (g)–(j) plot mean firing rate before (black) and after (red and blue) presentation of the adaptor, but in the absence of any post-test. Panels (k)–(o) show change (with respect to baseline) in firing rate (spikes s^{-1}) during the beginning (between 100 and 300 ms) of the adapting phase (left) and change in directional gain after adaptation (right) for the entire V1 population ($n=20$ tested subregions in 10 neurons). Similar data is plotted in (p)–(t) for the H1 population (38 tested subregions in 20 neurons). Error bars show ± 1 s.e.m. in (f)–(j), and 95% confidence intervals in (k)–(t). See §2 for definition of Δ gain. Stars indicate statistical significance (NS, non-significant; * $p < 0.05$; ** $p < 0.005$; *** $p < 0.0005$) as different from 0 (t -test).

We repeated the same experiment, but now the high-contrast adaptor covered the whole monitor, except for the area that was stimulated in the previous experiment (d). Adaptation in preferred and anti-preferred directions now yield opposite effects (e): adaptation in the preferred direction compresses the directional tuning curve (here by 53%—blue), but anti-preferred adaptation expands the tuning curve (by 63%—red). Compression is equivalent to a reduction in directional gain and expansion is equivalent to an increase (Treue & Martínez-Trujillo 1999). While the directional gain reduction in (c) is analogous to the contrast gain reduction previously reported for a similar class of fly neurons (Harris *et al.* 2000), the directional gain

enhancement in (e) (which resembles the effect of attention on macaque MT neurons; Treue & Martínez-Trujillo 1999) has not been described before. Clearly, the relative spatial positions of adaptor and test play an important role in adaptation that was not exposed in previous studies. This spatial effect on adaptation is not confined to the neuron H1. Lower panels (f)–(j) show similar data for the extensively characterized neuron V1 (Hausen 1984), which prefers downward motion in the frontolateral visual field. When the adapting stimulus is confined to the test region (g), adaptation in both the preferred and anti-preferred directions compresses the tuning curve (by 86% and 53%, respectively, (h)).

However, when the adaptor stimulates a wide area that excludes the test (*i*), preferred and anti-preferred adaptors have opposite effects: a compression of 53% for preferred and an expansion of 70% for anti-preferred (*j*).

(b) Full-field adaptors

What happens when the adaptor stimulates both the test region and regions outside the test (figure 2)? We selected a subregion (circled in (*a*)) within the response map of another V1 neuron. Panel (*f*) shows pre- and post-test (black and green, respectively) for a control condition in which nothing was presented during the adapting period. Adaptors in (*b*) and (*c*) correspond to the two conditions shown in figure 1 (curve is compressed by 61% in (*g*) and expanded by 32% in (*h*) for anti-preferred direction adaptation). Adaptors in (*d*) and (*e*) stimulated the entire area of the receptive field covered by the monitor. In (*d*), motion was uniform all over, whereas in (*e*) the area inside the tested subregion moved in opposite directions from the area outside. In both cases, directional tuning curves are compressed (by 19% (preferred) and 21% (anti-preferred) in (*i*), and by 23 and 48% in (*j*)). Expansion (directional gain enhancement) is only observed when (1) the region outside the test area is adapted in the anti-preferred direction and (2) the region inside the test area is left unadapted (adaptor in (*c*)).

Some of the effects of adaptation on directional tuning curves resemble the shifts and gain changes observed in previous studies of adaptation in both mammalian (Movshon & Lennie 1979; Carandini & Ferster 1997) and fly neurons (Harris *et al.* 2000). Our data confirm that shifts oppose recent activity in the cell, independent of the spatial relationship between adaptor and test (Harris *et al.* 2000), as seen in figure 1*h, j*, where preferred-direction adaptors (which increase firing rate during stimulation) shift the tuning curve (blue) downwards, whereas anti-preferred-direction adaptors (which reduce firing rate) produce an upward shift. This dependence on recent activity is true regardless of the spatial structure of the adaptor (i.e. similar shifts are observed in (*h*) and (*j*)). In figure 2, shifts in the tuning curves can be directly compared with shifts in the ongoing activity following adaptation (dotted lines), already measured by previous investigators (Srinivasan & Dvorak 1979; Harris *et al.* 2000). The shifts reflect a different mechanism from compression/expansion effects of the directional tuning curves, which represent changes in directional sensitivity (the response range spanned by the directional tuning curve) and have already been described as gain changes (Treue & Martínez-Trujillo 1999). Unlike the shifts, the changes in gain that compress and expand the tuning curves depend on the relative positions of adaptor and test. In the rest of the paper, we focus on this previously unreported effect of adaptation: the spatially dependent enhancement in directional gain.

(c) Directional gain analysis in V1 and H1

We quantified compression/expansion of directional tuning curves in our set of recordings by averaging directional gain change (see §2) across cells and tested locations, reported on the right of panels (*k*)–(*o*) in figure 2 for each test/adapt condition (shown by grating) for our V1 population. Similar data is plotted for the H1 population in panels (*p*)–(*t*). To show that the dependence

of adaptation effects on the location of the adapting stimulus cannot be attributed to differences in firing rate at different locations, we also report the response change elicited by the adaptor on the left of each panel. All of the preferred-direction adaptors produced similar increases in firing rate (blue), and all of the anti-preferred produced similar decreases (red). However, the gain changes subsequently produced by equally effective adaptors still depended on the spatial relationship between adaptor and test. For example, moving in the anti-preferred direction the adaptor in (*d*) reduces directional gain (red data point on the right side of panel (*n*)), whereas the adaptor in (*c*) enhances it by 19% on average (greater than 0 *t*-test, $p < 0.005$; greater than control paired *t*-test, $p < 0.05$). Similarly, H1 shows an average gain enhancement of 13% for adaptation in the anti-preferred direction outside the tested region (panel (*r*): greater than 0 *t*-test, $p < 0.0005$; greater than control paired *t*-test, $p < 0.05$). There was some variability in the effects we observed, mainly because our stimuli covered slightly different regions of the receptive field in each fly. Moreover, we found cases in which, for the same neuron, some locations within the receptive field showed clear directional gain enhancement effects, but others showed no effect. These variations are not surprising given the heterogeneous structure of these receptive fields (Krapp & Hengstenberg 1997; see vector response maps in figures 1–3).

Some of the data in figure 2 (panels (*m*)–(*o*)) suggest a simple physiological explanation for gain enhancement and depression. The adaptor in figure 2*c* must be influencing the overall excitability of the cell (possibly by adding or subtracting a dc potential at the spike initiation zone), resulting in the ‘rebound’ effect mentioned previously (Srinivasan & Dvorak 1979) and demonstrated by the dotted lines in figure 2*g–j*. The effect reported in panel (*m*) may then be explained by positing that changes in overall excitability are accompanied by similar changes in directional gain: when the neuron’s excitability is decreased by previous stimulation in the preferred direction, directional gain is similarly decreased (blue); when excitability is increased by previous stimulation in the anti-preferred direction, directional gain is similarly increased (red). This global mechanism, which is directionally selective in the sense that it depends on the direction of the adaptor, would act in combination with a second, local mechanism, whereby directional gain at a previously stimulated location would always be reduced regardless of the direction of the local adaptor, similarly to what Harris *et al.* (2000) reported for contrast gain. The latter mechanism would explain why the directional gain values in panel (*m*) are reduced in panels (*n*)–(*o*) by the addition of adaptation inside the test region (adaptors in (*d*)–(*e*)), regardless of the direction of this added adaptation. However, this explanation fails to account for the effects of adaptation within the test region only (with no adaptor outside), as reported in panel (*l*). In this case, one would still expect to see a contribution from both mechanisms, because the adaptor in (*b*) effectively drives the cell and thus modifies its overall excitability (see the change in response on the left of panel (*l*)). The change in excitability should then result in different gain changes for preferred and anti-preferred direction adaptation. Contrary to this prediction, the change in directional gain was identical for both directions of adaptation, in both V1 and

H1 (right sides of panels *(l)* and *(q)* in figure 2; paired *t*-tests for differences in gain changes between the two directions of adaptation were non-significant in both classes of neurons). We conclude that, although it is possible that the above explanation may be modified to provide a satisfactory interpretation of the effects we report, its most obvious formulation fails to account for our results.

(d) Patch-versus-patch experiment

A final experiment demonstrates that the interaction between areas of the receptive field is reciprocal. Our protocol resembles one previously adopted for studying macaque MT neurons (Kohn & Movshon 2003). We selected two separate areas within the receptive field and tested all four combinations of test and adapt locations. Figure 3 shows results for four V1 neurons. There are four panels for each neuron. When adaptation and testing are performed at the same location (upper-left and lower-right panels in *(a)*, and similarly for the other three neurons), both preferred and anti-preferred directions reduce directional gain (by, respectively, 55% and 45% on average for the four neurons). However, when different areas are adapted and tested (upper-right and lower-left panels), adaptation in the anti-preferred direction (red) leads to directional gain enhancement (by 18% on average), irrespective of which of the two areas is the adaptor (preferred direction causes an average compression of 7%).

We emphasize that this sensitization of one part of the receptive field by adaptation of another cannot be explained by the structure of the unadapted receptive field. The unadapted receptive fields of V1 and H1 do not display opponency (Hausen 1984; Krapp & Hengstenberg 1997). If they were opponent, the response to a subregion moving in the preferred direction (blue data point on left-hand side of figure 2*l*) should be reduced by surrounding motion in the same direction (blue point on left-hand side of figure 2*n*), and enhanced by a surround moving in the opposite direction (red point on left-hand side of figure 2*o*). We observed the exact opposite, confirming that there is no opponency. Interestingly, we noticed that our main effects were more robust in V1 than in H1. We think these differences are related to differences in the connectivity of these two neurons. H1 receives direct retinotopic input from the medulla (Hausen 1984), whereas V1 receives indirect input via three non-spiking neurons (Kurtz *et al.* 2001; Haag & Borst 2004). This suggests that spatially dependent directional gain adjustment may be the product of network interactions within the lobula plate, rather than earlier processing.

4. DISCUSSION

H1 and V1 are two major motion-sensitive spiking neurons in the fly lobula plate (Hausen 1984) with large receptive fields that are matched filters for patterns of optic flow (Krapp & Hengstenberg 1997). When a restricted region within the receptive field is exposed to high-contrast stimuli moving in either the preferred or anti-preferred direction, contrast gain is equally reduced (Harris *et al.* 2000). We showed that the same is true for directional gain (figure 2*l,q*). However, when the high-contrast adaptor stimulates regions outside the test region,

directional gain is either reduced or enhanced, depending on whether the adaptor moves in the preferred or anti-preferred direction, respectively (figure 2*m,r*). When the adaptor is located both within and outside the test region, the effect on directional gain is a combination of the two recalibration mechanisms just described (figure 2*n,o,s,t*).

How do these results relate to previous findings? Both in fly (Maddess & Laughlin 1985) and macaque (Kohn & Movshon 2003) motion-sensitive neurons, adaptation was shown to have no effect on contrast gain when adapted and tested regions do not overlap spatially. However, directional gain may change while leaving contrast gain unaffected. Moreover, we observed directional gain enhancement when the adaptor surrounding the test area was moving in the anti-preferred direction, and these previous studies only used the preferred direction. Thus, novel features of our experimental design have allowed us to observe an effect that had previously gone undetected. Although it remains to be confirmed whether effects similar to those we report here are also present in other neuronal types and animal species, there are good reasons to believe that our findings may extend to humans (Clifford & Langley 1996), as the influence of surround stimulation on the motion aftereffect has been clearly demonstrated psychophysically by several studies (Day & Strelow 1971; Anstis & Reinhardt-Rutland 1976; Murakami & Shimojo 1995). More specifically, surround motion can induce a stronger aftereffect within the central unadapted region than within the surround itself (Anstis & Reinhardt-Rutland 1976). This seemingly puzzling result from human psychophysics is perfectly consistent with our findings.

What useful function could this phenomenon serve? Adaptation eliminates redundancy and recalibrates the system for more efficient coding of novel events (Barlow 1990; Wainwright 1999; Brenner *et al.* 2000; Harris *et al.* 2000; Fairhall *et al.* 2001). Following this logic, directional gain should be modified at locations where no signal has been detected (the unadapted subregion) to emphasize novelty, 'motion is opposite to that observed elsewhere', and suppress the predictable 'motion carrying over in the same direction'. This interpretation is consistent with the effects we report, and would indicate that motion processing in H1 and V1 is dynamically adjusted to take into account potential discontinuities in the flow field. There is ample evidence that wide-field motion-sensitive neurons like H1 and V1 are involved in processing optic flow (Hausen 1984; Krapp & Hengstenberg 1996, 1997) and contribute to flight behaviour (Egelhaaf *et al.* 2002). During flight, proximal objects often generate behaviourally relevant discontinuities in the flow field as a consequence of motion parallax. Although H1 and V1 do not explicitly represent flow field discontinuities (Krapp & Hengstenberg 1997), our data indicate that their response characteristics may be recalibrated to take such discontinuities into account.

In summary, our results show that motion adaptation is more complicated than previously thought. A single neuron is capable of adjusting its response characteristics at a local level, by taking into account previous stimulation both locally within the receptive field and globally across the receptive field. Each subregion of the receptive field is dynamically recalibrated not only in relation to its own history, but also to that of surrounding regions. Our

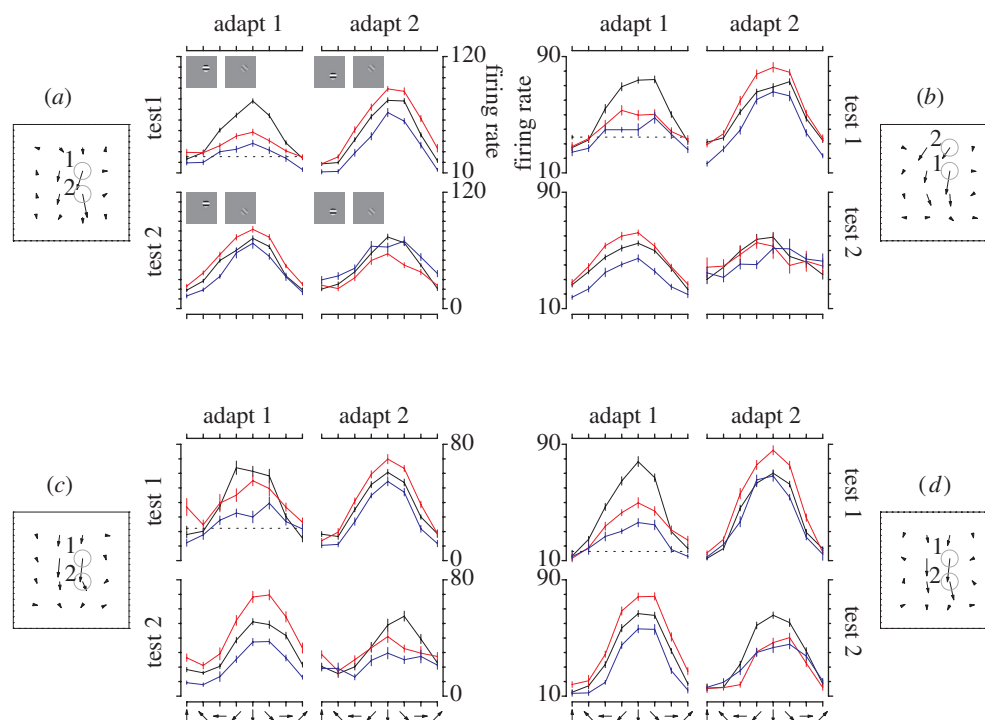


Figure 3. Patch-versus-patch experiment. For this experiment, we selected two subregions within each map (circled in (a)), and tested them separately (labelled as test 1 and test 2) before and after adapting to either the same or different location (labelled as adapt 1 and adapt 2). (a)–(d) plot data for four different V1 neurons, with four sub-panels each. When the tested region is adapted (top-left and bottom-right sub-panels), adaptation in both preferred (blue) and anti-preferred (red) directions leads to a reduction or no change in directional gain. When adaptation is performed at a different location (top-right and bottom-left sub-panels), the two directions display opposite effects on directional gain. Error bars show ± 1 s.e.m. Dotted lines are baseline firing rates (in the absence of visual stimulation).

experiments represent only a first step in the direction of uncovering new phenomena in gain recalibration and future experiments will need to elucidate the underlying cellular mechanisms.

We thank H. Barlow, H. Krapp, D. O'Carroll and S. Huston for comments. Supported by the Wellcome Trust (GR063322MA to P.N.).

REFERENCES

- Addams, R. 1834 An account of a peculiar optical phenomenon seen after having looked at a moving body. *Lond. Edinb. Phil. Mag. J. Sci.* **5**, 373–374.
- Anstis, S. M. & Reinhardt-Rutland, A. H. 1976 Interactions between motion aftereffects and induced movement. *Vis. Res.* **16**, 1391–1394. (doi:10.1016/0042-6989(76)90157-7.)
- Barlow, H. B. 1990 A theory about the functional role and synaptic mechanism of visual after-effects. In *Vision: coding and efficiency* (ed. C. Blakemore), pp. 363–375. Cambridge, UK: Cambridge University Press.
- Barlow, H. B. & Hill, R. M. 1963 Evidence for a physiological explanation of the waterfall phenomenon and figural aftereffects. *Nature* **100**, 1345–1347.
- Brenner, N., Bialek, W. & de Ruyter van Steveninck, R. 2000 Adaptive rescaling maximizes information transmission. *Neuron* **26**, 695–702. (doi:10.1016/S0896-6273(00)81205-2.)
- Carandini, M. & Ferster, D. 1997 A tonic hyperpolarization underlying contrast adaptation in cat visual cortex. *Science* **276**, 949–952. (doi:10.1126/science.276.5314.949.)
- Clifford, C. W. G. & Langley, K. 1996 Psychophysics of motion adaptation parallels insect electrophysiology. *Curr. Biol.* **6**, 1340–1342. (doi:10.1016/S0960-9822(02)70721-5.)
- Day, R. H. & Strelow, E. 1971 Reduction and disappearance of visual aftereffect of movement in the absence of patterned surround. *Nature* **230**, 55–56. (doi:10.1038/230055a0.)
- de Ruyter van Steveninck, R. R., Zaagman, W. H. & Masterbroek, H. A. K. 1986 Adaptation of transient responses of a movement-sensitive neuron in the visual system of the blowfly *Calliphora erythrocephala*. *Biol. Cybern.* **54**, 223–236. (doi:10.1007/BF00318418.)
- Egelhaaf, M., Kern, R., Hrapp, G. K., Kretzberg, J., Kurtz, R. & Warzecha, A.-K. 2002 Neural encoding of behaviourally relevant visual-motion information in the fly. *Trends Neurosci.* **25**, 96–102. (doi:10.1016/S0166-2236(02)02063-5.)
- Fairhall, A. L., Lewen, G. D., Bialek, W. & de Ruyter van Steveninck, R. R. 2001 Efficiency and ambiguity in an adaptive neural code. *Nature* **412**, 787–792. (doi:10.1038/35090500.)
- Götz, K. G. & Wenking, H. 1973 Visual control of locomotion in the walking fruitfly *Drosophila*. *J. Comp. Physiol.* **85**, 235–266.
- Haag, J. & Borst, A. 2004 Neural mechanism underlying complex receptive field properties of motion-sensitive interneurons. *Nat. Neurosci.* **7**, 628–634. (doi:10.1038/nn1245.)
- Harris, R. A., O'Carroll, D. C. & Laughlin, S. B. 2000 Contrast gain reduction in fly motion adaptation. *Neuron* **28**, 595–606. (doi:10.1016/S0896-6273(00)00136-7.)
- Hausen, K. 1984 The lobula-complex of the fly: structure, function and significance in visual behaviour. In *Photoreception and vision in invertebrates* (ed. M. A. Ali), pp. 523–559. New York: Plenum Press.
- Kohn, A. & Movshon, J. A. 2003 Neuronal adaptation to visual motion in area MT of the macaque. *Neuron* **39**, 681–691. (doi:10.1016/S0896-6273(03)00438-0.)

- Kohn, A. & Movshon, J. A. 2004 Adaptation changes the direction tuning of macaque MT neurons. *Nat. Neurosci.* **7**, 764–772. (doi:10.1038/nn1267.)
- Krapp, H. G. & Hengstenberg, R. 1996 Estimation of self-motion by optic flow processing in single visual interneurons. *Nature* **384**, 463–466. (doi:10.1038/384463a0.)
- Krapp, H. G. & Hengstenberg, R. 1997 A fast stimulus procedure to determine local receptive field properties of motion-sensitive visual interneurons. *Vis. Res.* **37**, 225–234. (doi:10.1016/S0042-6989(96)00114-9.)
- Kurtz, R., Warzecha, A. K. & Egelhaaf, M. 2001 Transfer of visual motion information via graded synapses operates linearly in the natural activity range. *J. Neurosci.* **21**, 6957–6966.
- Maddess, T. & Laughlin, S. B. 1985 Adaptation of the motion-sensitive neuron H1 is generated locally and governed by contrast frequency. *Proc. R. Soc. B* **225**, 251–275.
- Maffei, L., Fiorentini, A. & Bisti, S. 1973 Neural correlate of perceptual adaptation to gratings. *Science* **182**, 1036–1038.
- Mather, G., Anstis, S. & Verstraten, F. (eds) 1998 *The motion aftereffect: a modern perspective*. Cambridge, MA: MIT Press.
- Movshon, J. A. & Lennie, P. 1979 Pattern-selective adaptation in visual cortical neurones. *Nature* **278**, 850–852. (doi:10.1038/278850a0.)
- Murakami, I. & Shimojo, S. 1995 Modulation of motion aftereffect by surround motion and its dependence on stimulus size and eccentricity. *Vis. Res.* **35**, 1835–1844. (doi:10.1016/0042-6989(94)00269-R.)
- Srinivasan, M. V. & Dvorak, D. R. 1979 The waterfall illusion in an insect visual system. *Vis. Res.* **19**, 1435–1437. (doi:10.1016/0042-6989(79)90220-7.)
- Srinivasan, M. V., Jin, Z. F., Stange, G. & Ibbotson, M. R. 1993 ‘Vector white noise’: a technique for mapping the motion receptive fields of direction-selective visual neurons. *Biol. Cybern.* **68**, 199–207. (doi:10.1007/BF00224852.)
- Treue, S. & Martínez-Trujillo, J. C. 1999 Feature-based attention influences motion processing in macaque visual cortex. *Nature* **399**, 575–579. (doi:10.1038/21176.)
- Wainwright, M. J. 1999 Visual adaptation as optimal information transmission. *Vis. Res.* **39**, 3960–3974. (doi:10.1016/S0042-6989(99)00101-7.)

As this paper exceeds the maximum length normally permitted, the authors have agreed to contribute to production costs.